Downloaded from orbit.dtu.dk on: May 05, 2023

DTU Library

Multi-physical and multi-scale deterioration modelling of reinforced concrete part II: Coupling corrosion and damage at the structural scale

Lepech, Michael; Rao, Anirudh ; Kiremidjian, Anne; Michel, Alexander; Stang, Henrik; Geiker, Mette Rica

Published in:
Proceedings of fib Symposium 2015

Publication date:
2015

Document Version
Peer reviewed version

Link back to DTU Orbit

Citation (APA):
Lepech, M., Rao, A., Kiremidjian, A., Michel, A., Stang, H., & Geiker, M. R. (2015). Multi-physical and multi-scale deterioration modelling of reinforced concrete part II: Coupling corrosion and damage at the structural scale. In *Proceedings of fib Symposium 2015*

General rights
Copyright and moral rights for the publications made accessible in the public portal are retained by the authors and/or other copyright owners and it is a condition of accessing publications that users recognise and abide by the legal requirements associated with these rights.

- Users may download and print one copy of any publication from the public portal for the purpose of private study or research.
- You may not further distribute the material or use it for any profit-making activity or commercial gain
- You may freely distribute the URL identifying the publication in the public portal

If you believe that this document breaches copyright please contact us providing details, and we will remove access to the work immediately and investigate your claim.

MULTI-PHYSICAL AND MULTI-SCALE DETERIORATION MODELLING OF REINFORCED CONCRETE PART II: COUPLING CORROSION AND DAMAGE AT THE STRUCTURAL SCALE

Michael D. Lepech[1], Anirudh Rao[1], Anne Kiremidjian[1], Alexander Michel[2], Henrik Stang[2], and Mette Geiker[3]

[1]Department of Civil and Environmental Engineering, Stanford University, Stanford, California, 94305-4020, USA

[2]Department of Civil Engineering, Technical University of Denmark, Kgs. Lyngby, DK-2800, Denmark

[3]Department of Structural Engineering, Norwegian University of Science and Technology, Trondheim, NO-7491, Norway

Abstract

Deterioration of reinforced concrete infrastructure such as bridges, tunnels, and buildings represents one of the major challenges currently facing developed countries. This deterioration leads to economic costs for maintenance and replacement, environmental impacts such increased global warming potential as a result of cement production and traffic emissions, and social costs related to traffic congestion and human health concerns. While engineering tools and methods for structural modelling and design of new reinforced concrete infrastructure are mature, the methods and tools for modelling decades-long deterioration and maintenance are much less developed. An approach for modelling structural deterioration of reinforced concrete components due to reinforcement corrosion is presented and a procedure is introduced to estimate the time-dependent structural response, described using time-dependent seismic fragility curves. The approach is part of a multi-disciplinary framework which includes physical, chemical, and electrochemical processes at the meso-scale coupled with mechanical deterioration processes, which are modelled using finite element methods, at the macro-scale. While not detailed in this paper, when the time-dependent assessment of structures is integrated with life cycle assessment models that quantify the economic, environmental, and social impacts of infrastructure, the result is a comprehensive assessment methodology for the sustainability of deteriorating reinforced concrete infrastructure.

Keywords: Service Life Modelling, Concrete Deterioration, Multi-Scale Model, Multi-Physical Model, Sustainability

1 Introduction

Deterioration of reinforced concrete infrastructure such as bridges, tunnels, and buildings represents one of the major challenges currently facing developed countries. (ASCE 2013, Giorno 2011, OECD 2011) This deterioration leads to economic costs for repair, maintenance, and replacement of infrastructure, environmental impacts such increased global warming potential as a result of cement production and traffic emissions, and social costs related to traffic congestion and human health concerns. (Lepech *et al*. 2014) Much of this infrastructure is built from reinforced concrete. While engineering tools and methods for structural modelling and design of new reinforced concrete infrastructure are mature, the methods and tools for modelling decades-long deterioration and maintenance are much less developed. The methods and tools that exist for predictive deterioration

modelling often focus on a single scale (*i.e.* material deterioration or structural deterioration) and a single phenomenon (*i.e.* moisture ingress leading to freeze thaw deterioration or chloride ingress leading to reinforcement corrosion). (*e.g.* Liu & Weyers 1998, Jensen *et al.* 2012, Schlangen & Copuroglu 2005) This is due to the highly complex nature of deterioration in reinforced concrete, which involves coupled physical phenomena that are present at a range of scales. Because of this complexity, the future performance of designs is difficult to determine and efforts to engage in more sustainable infrastructure design are handicapped.

In this paper, an approach for modelling structural deterioration of reinforced concrete bridge components due to reinforcement corrosion is presented and a procedure is introduced to estimate the time-dependent structural response using time-dependent fragility curves. The multi-disciplinary framework presented is based on physical, chemical, and electrochemical processes at the meso-scale coupled with mechanical deterioration processes, which are modelled using finite element methods, at the macro-scale. Finite element method (FEM) models are used to link corrosion of steel reinforcement, including electrochemical processes at the reinforcement surface, with loss of structural capacity of a reinforced concrete column element. The individual FEM models, built in COMSOL and OpenSees, are coupled through exchange of section properties (i.e. remaining rebar cross section, presence of cover cracking) along the height of the column. The overall multi-physical and multi-scale modelling framework is shown schematically in Figure 1. The focus of this paper is the formulation of the "Structural Performance Module" shown in the upper left portion of Figure 1.

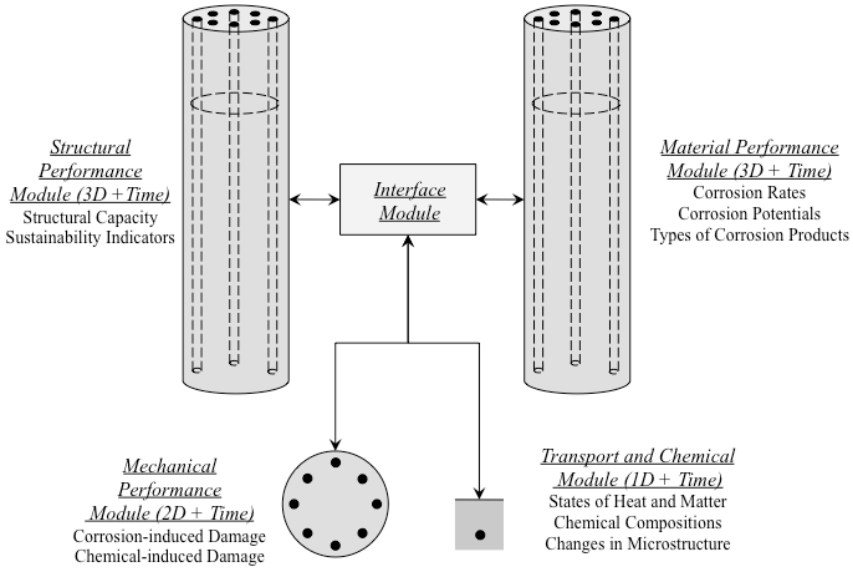

Fig. 1 Multi-physical and multi-scale reinforced concrete deterioration modelling architecture. The focus of this paper is the formulation of the "Structural Performance Module" shown in the upper-left of Figure 1.

2 Linking Multiple Scales in Reinforced Concrete Deterioration Modelling

The material-scale reinforcement corrosion model is based on physical laws describing the thermodynamics and kinetics of electrochemical processes including activation, resistance, and concentration polarisation, as well as the impact of temperature, relative humidity, and oxygen. (Michel *et al.* 2013) Building off of such "materials performance" modelling, a structural-scale performance model ("Structural Performance Module" in Figure 1) is the focus of this paper. Such a model is a critical, often missing, link between the vast literature focusing on concrete deterioration and steel reinforcement corrosion and infrastructure capacity and reliability assessments and actionable decision-making.

Corrosion of reinforcement damages reinforced concrete structures in multiple ways. First, the cross sectional area of both longitudinal and transverse steel is reduced due dissolution of iron. Second, expansive oxidation products generate tensile stresses in the surrounding concrete, which lead to cracking of the concrete cover. Third, the formation of these cracks leading up to the surface leads

to an acceleration of the local rate of corrosion, causing localized reduction in steel cross-section. This can cause localized strain peaks in the steel, resulting in a loss of ductility in the structure. Finally, the cover cracking and spalling leads to a reduction in the concrete cross-sectional area. It is the loss of reinforcing steel cross sectional area and reductions in the concrete cross-sectional area along a reinforced concrete member that forms the computational link between the "Material Performance Modules" (Mechanical Performance and Service Life Prediction Modules) and the "Structural Performance Module" in Figure 1. This link is shown schematically in Figure 2.

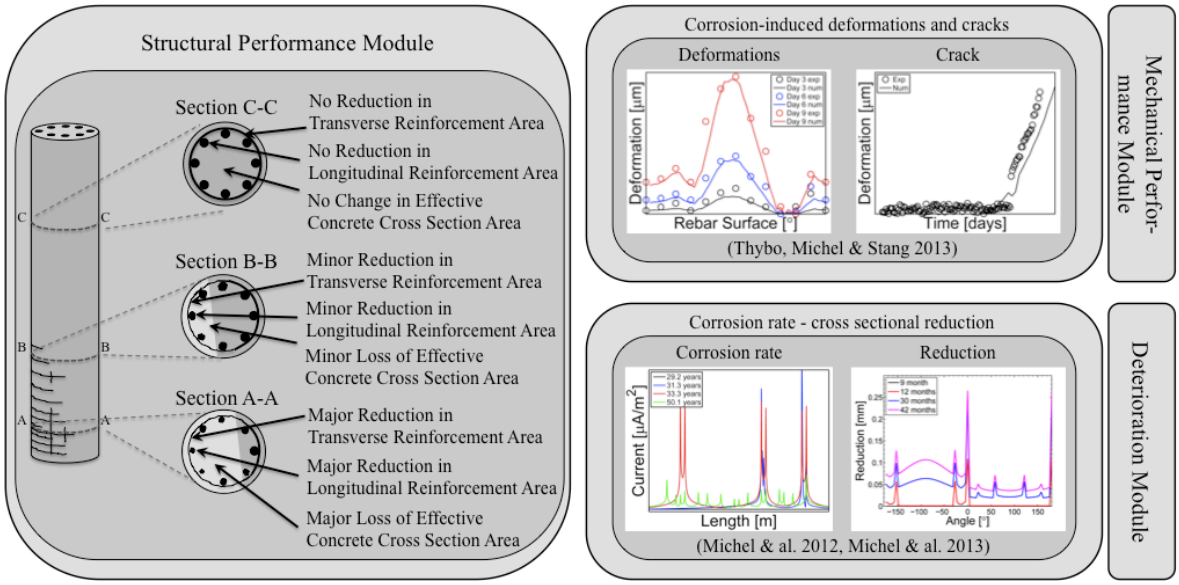

Fig. 2 Schematic representation of computational link between the Material Performance Modules (Mechanical Performance and Service Life Prediction Modules) and the Structural Performance Module. Computation links are the cross sectional areas of longitudinal reinforcing steel bars, transverse reinforcing steel bars, and effective concrete area. These values are determined along the length of the member.

2.1 Deterioration Phenomena Considered in Structural Performance Modelling

In addition to the reduction of longitudinal and transverse reinforcement cross sectional areas and cracking through the concrete cross section along the member length (Figure 2), a number of other phenomena are also considered in the structural performance model. These include (1) cracking and spalling of the concrete cover, (2) change in reinforcement bond strength due to formation of oxidation products, (3) reduction in capacity of corroded reinforcing bars, (4) reduction in ductility of corroded reinforcing bars, and (5) buckling of corroded reinforcing bars. Each model implemented within the larger structural performance module is described in more detail.

The cracking and spalling of the cover concrete caused by the expansive rust products can be captured by reducing the strength of the cover concrete elements using the model described by Coronelli & Gambarova (2004) and Molina *et al.* (1993) and shown in Equations 1 through 3.

$$f_c^* = \frac{f_c^{'}}{1 + \frac{\kappa \varepsilon_1}{\varepsilon_{co}}} \tag{1}$$

$$\varepsilon_1 = \frac{D_{ele}^* - D_{ele}}{D_{ele}} \tag{2}$$

$$D_{ele}^* - D_{ele} = n_{bars} w_{cr} = 2\pi n_{bars} (\nu_{r/s} - 1) x \tag{3}$$

where, f'_c is the original strength of the concrete cover elements, κ is a parameter related to bar diameter and roughness ($\kappa \sim 0.1$ for medium diameter deformed bars), ε_{co} is the strain at peak compressive stress, D_{ele} is the diameter of the element before cracking, D^*_{ele} is the diameter of the element after cracking, n_{bars} is the number of longitudinal rebars undergoing compression, w_{cr} is the sum of the widths of all crack openings for a given corrosion level, $\nu_{r/s}$ is the ratio between the specific volumes of rust and steel, and x is the depth of penetration of the corrosives into the element section.

The reduction in reinforcement steel diameter, the loss of confinement due to cracking and spalling of the concrete cover and formation of porous rust products at the steel-concrete interface may also lead to changes in the bond-strength between steel and concrete. Several experimental tests have been conducted to study the influence of corrosion on bond strength (e.g. Al-Sulaimani *et al.*1990, Cabrera 1996, Almusallam *et al.* 1996, Stanish *et al.* 1999, Amleh & Mirza 1999, Hassan 1999, Castel *et al.* 2000, Auyeung *et al.* 2001, Lee *et al.* 2002, Fang *et al.* 2004, Wang & Liu 2004, Fang *et al.* 2006). However, there are large variations in the change in bond strength as a function of degree of corrosion as reported by these various experimental studies. For instance, as noted by Fang *et al.* (2004) and Wang & Liu (2004), the effects of corrosion on bonding in well confined concrete are negligible. On the other hand, Amleh & Mirza (1999) and Fang *et al.* (2006) report that the bond strength decreases substantially at higher levels of corrosion, whereas Berra *et al.* (1997) noted a moderate increase in bond strength with increasing corrosion when efficient skin reinforcement was provided in order to confine the bars. Based on existing literature, no clear relationship between the bond strength and corrosion level can be ascertained. There is also a lack of theoretical models that can correctly predict the loss in bond strength due to corrosion. Due to these reasons, certain assumptions have to be made in order to study the effect of corrosion on the bond between the rebar steel and concrete. A comparison of residual bond strength at different levels of corrosion show an increase in bond strength at lower levels of corrosion (less than 2% cross sectional area loss), which is assumed to be negligible. With further increase in the level of corrosion, the bond strength is shown to decrease according to an empirical equation shown as Equation 4. (*fib* 2000)

$$\tau^*_{\max} = \begin{cases} \tau_{\max} & \text{if } X < 2\% \\ 1.5\tau_{\max} X^{-0.6} & \text{if } X > 2\% \end{cases} \tag{4}$$

where, τ^*_{max} is the residual bond strength after corrosion, τ_{max} is the bond strength before corrosion, and X is the cross section area loss.

Du *et al.* (2005a, 2005b) conducted an experimental study of laboratory corroded reinforcement specimens to identify the cause and mechanism of the reduction in the yield and ultimate strength of corroded reinforcement, and to determine the extent of this reduction. They proposed Equations 5 through 7 for determining the yield strength, ultimate strength, and ultimate strain of corroded bars, respectively.

$$f_y = (1 - 0.005x) f_{yo} \tag{5}$$
$$f_u = (1 - 0.005x) f_{uo} \tag{6}$$
$$\varepsilon_u = (1 - 0.005x) \varepsilon_{uo} \tag{7}$$

where, f_y, f_u, and ε_u are the yield strength, ultimate strength, and ultimate strain of corroded reinforcement, respectively, x is the amount of steel mass loss due to corrosion in percent, and f_{yo}, f_{uo}, and ε_{uo} are the yield strength, ultimate strength, and ultimate strain of non-corroded reinforcement, respectively.

Due to the spalling of concrete cover that often occurs as a result of corrosion, certain lengths of corroded reinforcement suffer from a lack of confinement, making these bars more likely to buckle in compression. If the length of the unsupported portion of the corroded bar and its reduced diameter are known, the critical buckling stress for the corroded bar can be calculated using Euler's equation shown as Equation 8 (Tapan & Aboutaha 2008).

$$f_{crit} = \frac{\pi^2 E_s(x) I_b(x)}{L_{\exp}^2 A_b(x)} \tag{8}$$

where, f_{crit} is the critical buckling stress of the corroded reinforcement, x is the amount of steel mass loss due to corrosion in percent, $E_s(x)$ is the elastic modulus of the corroded reinforcement, $I_b(x)$ is the moment of inertia of the corroded reinforcement, $A_b(x)$ is the cross-sectional area of the corroded reinforcement, L_{exp} is the unsupported length of the corroded reinforcement.

2.2 Structural Modelling of a Corroded Reinforced Concrete Member

The analytical modelling of a corroded element is conducted using the Open System for Earthquake Engineering Simulation (OpenSees) software (Mazzoni *et al.* 2007), a finite element method based object oriented software framework for simulating the seismic response of structural systems. OpenSees was chosen because it provides an extensive library of material models, non-linear elements and solvers that can be easily interchanged, and it has been widely adopted by the research community, making it highly conducive for the modelling and simulation of complex structural systems subject to dynamic loading. The element is modelled as a nonlinear distributed-plasticity fiber beam-column element, which is a flexibility-based element that considers the spread of plasticity along the length of the element.

The reinforcement steel is modelled using the uniaxial Giuffre-Menegotto-Pinto 'Steel02' material, which provides isotropic strain hardening. As corrosion occurs, the material changes discussed in Section 2.1 are applied. The confined core concrete fibers and unconfined cover concrete fibers are modelled using the uniaxial 'Concrete01' material in OpenSees, which provides a parabolic stress-strain response for the concrete in compression up to the maximum compressive strength, beyond which the strength deteriorates linearly to a residual strength. Concrete01 provides no tensile strength. As corrosion occurs, the material changes discussed in Section 2.1 are applied. The original maximum compressive strength of the confined concrete and the corresponding strain are calculated using the theoretical stress-strain model proposed by Mander *et al.* (1988) and shown as Equations 9 and 12.

$$f_{cc}^{'} = f_{co}^{'}\left(-1.254 + 2.254\sqrt{\frac{1 + 7.94 f_t^{'}}{f_{co}^{'}}} - 2\frac{f_t^{'}}{f_{co}^{'}}\right) \tag{9}$$

$$\varepsilon_{cc} = 0.002\left(1 + 5\left(\frac{f_t^{'}}{f_{co}^{'}} - 1\right)\right) \tag{10}$$

$$f_t^{'} = 0.5 k_e \rho_s f_{yh} \tag{11}$$

$$k_e = \frac{1 - \frac{s^{'}}{2d_s}}{1 - \rho_{cc}} \tag{12}$$

where, f'_{cc} is the confined concrete strength, f'_{co} is the unconfined concrete strength, f'_t is the confining lateral pressure provided by the transverse reinforcement, f_{yh} is the yield strength of the transverse reinforcement, ρ_s is the transverse reinforcement ratio, ρ_{cc} is the ratio of longitudinal rebar cross sectional area to the area of the concrete core, s' is the clear spacing of the transverse reinforcement, and d_s is the diameter of the concrete core.

An elastic shear section is combined with the section of the beam-column element to capture the shear component of the total deflection of the element that is calculated using elastic theory as shown in Equation 13.

$$\Delta_{shear} = \frac{4}{3}\left(\frac{VH_{ele}}{GA_G}\right) \tag{13}$$

where, Δ_{shear} is the total deflection of the element due to shear, H_{ele} is the height or length of the element, A_G is the cross sectional area of the element, G is the shear modulus of concrete.

The typical assumption of a perfect bond between the longitudinal steel and concrete neglects the slippage of the anchorage section of the steel, making the beam-column element appear stiffer than it is in reality. Thus a zero-length section is introduced at one end of the element to account for the component of the deformation due to bond-slip. The zero-length element is defined by a master-node and a slave-node at the same location. The master-node has all degrees of freedom restrained and the slave-node has its translational degrees of freedom constrained to be equal to those of the master node. This zero-length section has the same number of steel and concrete fibers as the non-linear beam-column element sections above it. The tensile stress-displacement model used for the reinforcement is based on the three-parameter bond-stress model (Ranf 2007). As done for material properties, as corrosion occurs the changes to reinforcement bond as discussed in Section 2.1 are applied.

3 Structural Deterioration Model Validation

In order to validate the assumptions made in the corrosion modelling approach described above, analytical and experimental test results of several reinforced concrete columns were compared. Two separate sets of experimental tests are used for validation of the structural modeling of corroded reinforced concrete columns. The first set of tests comprised eight columns having the same specifications, which were subjected to different axial loads and varying degrees of accelerated corrosion in an experimental study conducted at the State Key Laboratory of Coastal and Offshore Engineering at Dalian University of Technology in China (Li & Gong 2008).

The experimental reinforced concrete column test studies undertaken by Li & Gong (2008) were 1m tall and had a diameter of 0.26m. The longitudinal reinforcement consisted of 6m x 16m bars. The transverse reinforcement consisted of 8mm stirrups at a spacing of 0.1m. The concrete cover was 0.03m. Corrosion was induced in the test specimens through the application of an external current. The specimens to be corroded were placed in a 3.5% NaCl solution and a current of 1.0 mA/cm^2 was applied with a corrosion resistant plate immersed in the solution serving as the cathode and the reinforcement serving as the anode. At the end of the accelerated corrosion process, longitudinal cracks were observed running parallel to the steel bars in the corroded column specimens, and the authors noted that the corrosion damage was uniform along the length of the bars. A constant axial load was applied using hydraulic jacks. Table 1 shows the different axial load ratios and corrosion mass loss ratios for the series of tested column specimens. The corroded and non-corroded test columns were subjected to reversed cyclic loading using a triangular waveform.

Table 1 Axial load ratios and mass loss ratios for corroded column experimental test series by Li & Gong (2008)

Specimen	A		B			C		D
	A_0	A_{12}	B_0	B_{21}	B_{22}	C_0	C_{32}	D_{43}
Mass loss due to corrosion (%)	0.00%	9.40%	0.00%	5.10%	9.40%	0.00%	9.40%	14.70%
Axial Load Ratio (ALR)	0.15			0.25		0.40		0.32

The hysteresis curves obtained from the experimental tests (red lines) and the corresponding OpenSees analyses (blue lines) for the specimens A_0, A_{12}, B_0, and B_{22} are plotted in Figures 3 through 6. The mean error in hysteretic force calculated was 12.9% and the mean absolute error in hysteretic energy was 25.3%. These error values are lower than the corresponding values reported by Berry & Eberhard (2007) in their validation of the OpenSees modelling software, indicating that this analytical model of corroded reinforced concrete elements is able to provide a similar degree of accuracy as the model proposed by Berry & Eberhard (2007) for noncorroded elements. Column specimen D_{43}, which was subjected to a high axial load ratio (0.32) coupled with a high degree of corrosion (14.7% steel

mass loss) was the source of the highest error in both hysteretic force (15.97%) and hysteretic energy (53.21%). However, this specimen was tested as an extreme case and the combination of such a high axial load ratio and degree of corrosion is unlikely to be seen in an actual structural element. The hysteresis curves from the experimental tests are not symmetrical about the load axis. This is due to higher lateral deformations and earlier yielding of one side of the element as compared to the other. This asymmetric behavior cannot be predicted by the material models used in the analytical model.

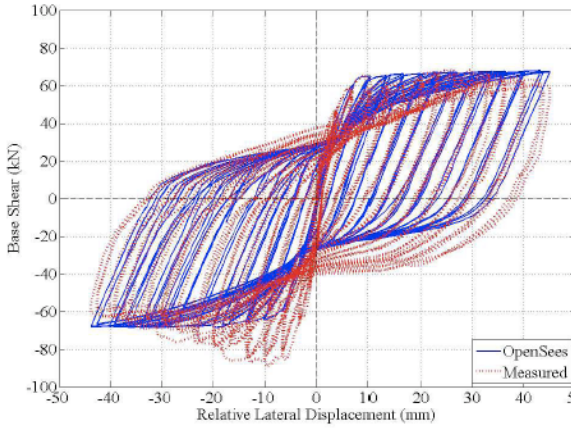

Fig. 3 Comparison of experimental (red) and modelled (blue) hysteresis curves (base shear vs. lateral displacement) for column A_0

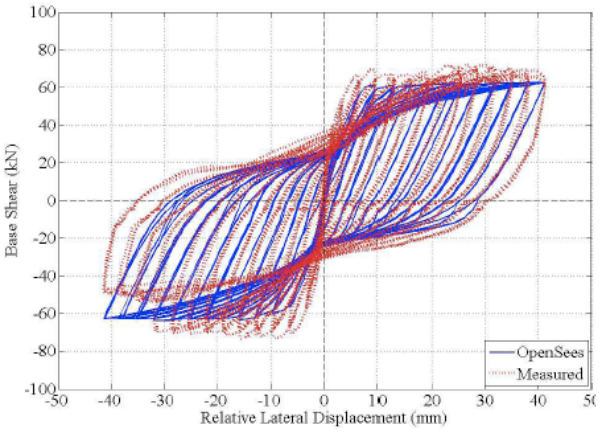

Fig. 4 Comparison of experimental (red) and modelled (blue) hysteresis curves (base shear vs. lateral displacement) for column A_{12}

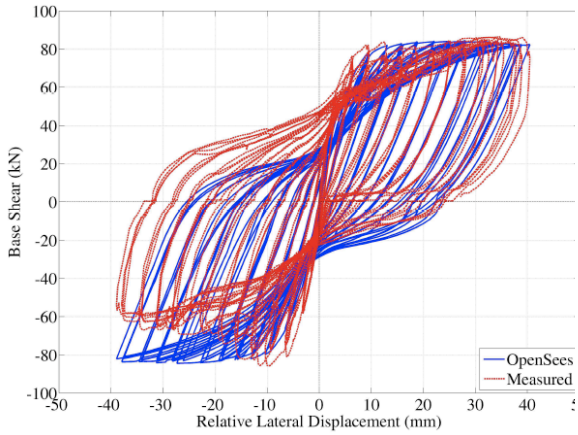

Fig. 5 Comparison of experimental (red) and modelled (blue) hysteresis curves (base shear vs. lateral displacement) for column B_0

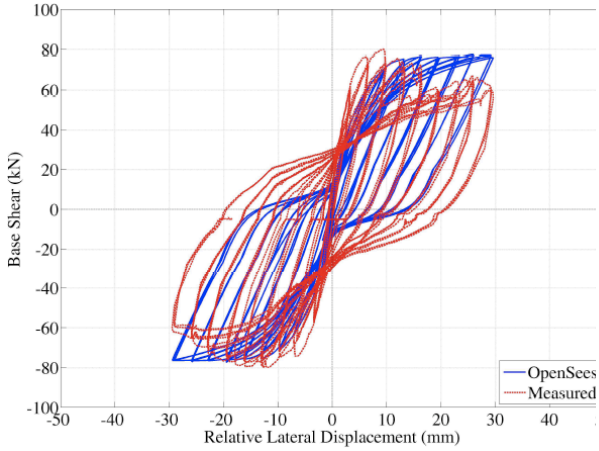

Fig. 6 Comparison of experimental (red) and modelled (blue) hysteresis curves (base shear vs. lateral displacement) for column B_{22}

4 Fragility of Corroded Reinforced Concrete Elements

Fragility analysis involves understanding and probabilistically quantifying the liklihood of a structure or structural component to undergo damage during severe loading (i.e. an earthquake). Fragility analysis forms an integral part of the Pacific Earthquake Engineering Research (PEER) Center framework for seismic risk analysis, along with seismic hazard analysis and consequence analysis. As a result, much work has been done in the past two decades to develop methods to generate fragility functions for both structural and non-structural components. However, the onset of corrosion deterioration can lead to a shifting of the fragility curves for a component over time, contributing to a time-dependent seismic risk for the component. Thus, this paper introduces a method of address the effects of deterioration on the fragility of structures.

The construction of analytical fragility curves for structural components involves both the damage state capacities, C_i, and the demand generated on the component as a function of load (ground

motion intensity), D(im). These are modelled analytically, and the fragility function corresponding to the i^{th} damage state of the element can be described as Equations 14 and 15.

$$Fr_i(im) = P\left[D(im) \geq C_i\right] \tag{14}$$

$$Fr_i(im) = P\left[\frac{D(im)}{C_i} \geq 1\right] \tag{15}$$

where, $Fr_i(im)$ is the probability that the i^{th} damage state of the element will be met or exceeded. The structural capacity and seismic demand are often modelled using lognormal distributions. In this case, the probability that a particular damage state will be met or exceeded will also be described by a lognormal CDF as shown in Equation 16.

$$Fr_i(im) = \Phi\left[\frac{\mu_{\ln D(im)} - \mu_{\ln Ci}}{\sqrt{\beta^2_{D(im)} + \beta^2_{C_i}}}\right] \tag{16}$$

where, $\mu_{\ln D(im)}$ is the mean of the natural logarithm of the seismic demand at an intensity level im, $\mu_{\ln Ci}$ is the mean of the natural logarithm of the ith damage state capacity, $\beta_{D(im)}$ is the logarithmic standard deviation of the seismic demand at an intensity level im, β_{Ci} is the logarithmic standard deviation of the i^{th} damage state capacity, Φ is the standard normal distribution function.

The severity of damage in reinforced concrete elements following an earthquake is usually categorized in terms of discrete damage states. The delineation between the damage states is typically based on the consequences the damage is likely to entail, such as the type and cost of repair actions required to bring the damaged component back to its original undamaged state. Mackie *et al.* (2008) proposed four damage states corresponding to (1) initial cracking, (2) cover spalling, (3) longitudinal bar buckling in the element, and (4) element failure.

The evolution of the damage state capacities with corrosion can be depicted graphically in the form of capacity surfaces. These surfaces depict the probability of exceeding a given damage state provided a known degree of corrosion in the element and the structural load. Figures 7 and 8 show the capacity surfaces for damage states 3 (longitudinal bar buckling in the element) and 4 (element failure) for reinforced concrete column designed according to the 1971-1990 era structural design code in California. Ultimately, these curves provide a probabilistic quantification of the increasing risk of failure of reinforced concrete elements due to increasing levels of reinforcement corrosion.

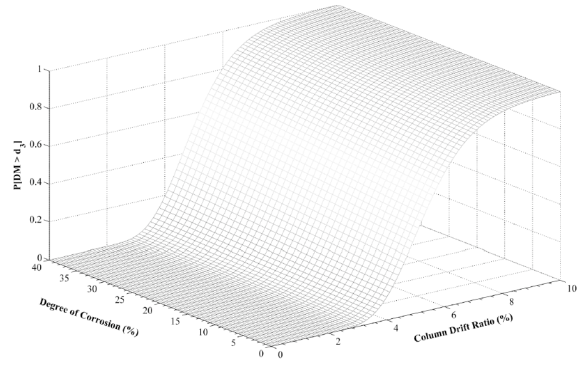

Fig. 7 Capacity surface for damage state 3 (longitudinal bar buckling in the element) for a reinforced concrete column designed to 1971-1990 era California design codes

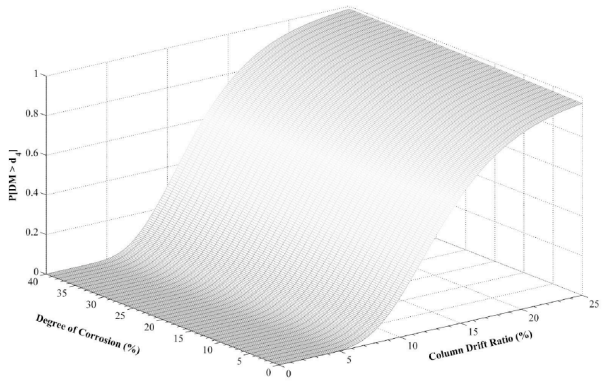

Fig. 8 Capacity surface for damage state 4 (element failure) for a reinforced concrete column designed to 1971-1990 era California design codes

Beyond multi-scale modelling of deterioration of reinforced concrete elements, this framework is intended to inform decision-makers interested in designing and managing reinforced concrete

infrastructure for reduced sustainability impacts over its decades-long service life. This requires the integration of multi-physical and multi-scale design and modelling tools with comprehensive life cycle assessment models. Such integration is shown schematically is Figure 9 and is the ultimate application driving development of this modelling framework.

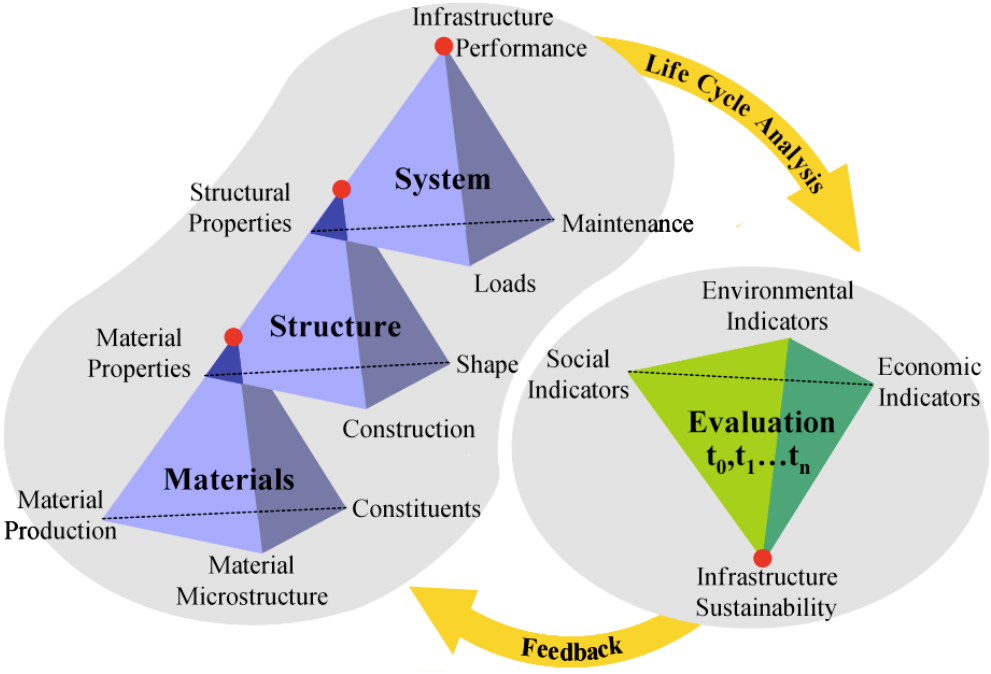

Fig. 9 Multi-scale design and modelling framework within the Sustainable Integrated Materials, Structures, Systems (SIMSS) Design Approach (Lepech 2006)

5 Conclusion

This paper presented the ”structural performance module” within a newly developed multi-physical and multi-scale modelling framework for corrosion in reinforced concrete elements. The structural performance module is linked computationally to a material performance module, which provides the cross sectional areas of longitudinal and transverse reinforcing steel bars and the effective concrete cross section along the length of the member. A number of other damage types are also considered, which include cracking and spalling of the concrete cover, change in reinforcement bond strength due to formation of corrosion products, reduction in capacity of corroded reinforcing bars, reduction in ductility of corroded reinforcing bars, and buckling of corroded reinforcing bars. When compared to experimental response of corroded reinforced concrete elements loaded in full hysteresis, the analytical model is able to provide the same degree of accuracy as models proposed for non-corroded elements.

Beyond modelling the structural effects of reinforced concrete corrosion, fragility analysis was shown to be a powerful tool for assessing the impact of reinforced concrete deterioration. Deterioration due to reinforcement corrosion causes a decrease in the median capacities for damage states ranging from initial cracking to failure of reinforced concrete elements. This decrease in median capacities can be captured by the use of the changed geometric and material properties of the deteriorating column in prescriptive equations for predicting the capacities. Ultimately, this analysis will be integrated within a full life cycle assessment to support comprehensive decision-making in order to minimize environmental, social, and economic impacts associated with the decades-long service life of reinforced concrete elements and structures.

Acknowledgements

The authors wish to acknowledge the support of the Stanford Blume Fellowship, the Stanford Terman Faculty Fellowship, and the Nordic Innovation Centre Project Number 08190 SR. This material is also based upon work supported by the United States National Science Foundation under Grant No. 1453881. Any opinions, findings, and conclusions or recommendations expressed in this material are those of the authors and do not necessarily reflect the views of the United States National Science Foundation.

References

Al-Sulaimani, G., M. Kaleemullah, I. Basunbul, and Rasheeduzzafar. (1990) Influence of corrosion and cracking on bond behavior and strength of reinforced concrete members. ACI Structural Journal, 87(2):220–231.

Almusallam, A.A., A. S. Al-Gahtani, A. R. Aziz, and Rasheeduzzafar. (1996) Effect of reinforcement corrosion on bond strength. Construction and Building Materials, 10(2): 123–129.

American Society of Civil Engineers ASCE. (2013), 2013 Report Card for America's Infrastructure. Committee on America's Infrastructure. American Society of Civil Engineers. March 2013. pp. 1-74. Source: http://www.infrastructurereportcard.org/a/documents/2013-Report-Card.pdf

Amleh, L. and S. Mirza. (1999) Corrosion influence on bond between steel and concrete. ACI Structural Journal, 96(3):415–423.

Auyeung, Y., P. Balaguru, and L. Chung. (2001) Bond Behavior of Corroded Reinforcement Bars. ACI Materials Journal, 97(2):214–221.

Berra, M., A. Castellani, and D. Coronelli. (1997) Bond in reinforced concrete and corrosion of bars. In 7th International Conference on Structural Faults and Repair, volume 2, pages 349–356, Edinburgh, UK, 1997. Engineering Technics Press.

Berry, M.P., and M. O. Eberhard. (2007) Performance modeling strategies for modern reinforced concrete bridge columns. Technical report, Pacific Earthquake Engineering Research Center, University of California, Berkeley, Berkeley, CA.

Cabrera. J. (1996) Deterioration of concrete due to reinforcement steel corrosion. Cement and Concrete Composites, 18(1):47–59.

Castel, A., R. François, and G. Arliguie (2000). Mechanical behaviour of corroded reinforced concrete beams—Part 2: Bond and notch effects. Materials and Structures, 33(9):545–551.

Coronelli , D. & P. Gambarova. (2004) Structural Assessment of Corroded Reinforced Concrete Beams: Modeling Guidelines. Journal of Structural Engineering, 130(8): 1214–1224.

Du, Y.G., A. Chan, and L. Clark. (2005a) Effect of corrosion on ductility of reinforcing bars. Magazine of Concrete Research, 57(7):407–419.

Du, Y.G., L. Clark, and A. Chan. (2005b) Residual capacity of corroded reinforcing bars. Magazine of Concrete Research, 57(3):135–147.

Fang, C., K. Lundgren, L. Chen, and C. Zhu. (2004) Corrosion influence on bond in reinforced concrete. Cement and Concrete Research, 34(11):2159–2167.

Fang, C., K. Lundgren, M. Plos, and K. Gylltoft. (2006) Bond behaviour of corroded reinforcing steel bars in concrete. Cement and Concrete Research, 36(10):1931–1938.

fib (2000). fib Bulletin No. 10. Bond of reinforcement in concrete. Technical report, International Federation for Structural Concrete (fib), Lausanne, Switzerland.

Giorno, C. (2011) Meeting Infrastructure Needs in Australia. Organisation for Economic Co-operation and Development (OECD). Working Paper No. 851. March 24, 2011. pp. 30. ISSN : 1815-1973

Hassan, A. (1999) Bond of Reinforcement in Concrete with Different Types of Corroded Bars. Master's thesis, Ryerson University.

Jensen, M.M., Johannesson, B., Geiker, M. (2012). "A coupled chemical and mass transport model for concrete durability". In: 8th Int. Conference on Engineering Computational Technology. Topping, B.H.V. (ed.). September 4-7, 2012. Dubrovnik, Croatia.

Lee, H-S., T. Noguchi, and F. Tomosawa. (2002) Evaluation of the bond properties between concrete and reinforcement as a function of the degree of reinforcement corrosion. Cement and Concrete

Research, 32(8):1313–1318.
Lepech, M. (2006) “A Paradigm for Integrated Structuers and Materials Design for Sustainable Transportation Infrastructure”PhD Thesis. Department of Civil and Environmental Engineering. University of Michigan, Ann Arbor. USA.
Lepech, M. D., Geiker, M., & Stang, H. (2014). Probabilistic design and management of environmentally sustainable repair and rehabilitation of reinforced concrete structures. Cement and Concrete Composites, Vol. 47, pp. 19-31.
Li, J. and J. Gong. (2008) Influences of Rebar Corrosion on Seismic Behavior of Circular RC Columns. China Journal of Highway and Transport, 21(4):55–60.
Liu, Y., & Weyers, R. E. (1998). Modeling the time-to-corrosion cracking in chloride contaminated reinforced concrete structures. ACI Materials Journal. Vol. 95, No. 6., pp. 675-680.
Mackie, K.R., J.-M. Wong, and B. Stojadinovi´c. (2008) Integrated Probabilistic Performance- Based Evaluation of Benchmark Reinforced Concrete Bridges. Technical Report January, Pacific Earthquake Engineering Research Center, University of California, Berkeley, Berkeley, CA.
Mander, J.B., M. Priestley, and R. Park. (1988) Theoretical Stress-Strain Model for Confined Concrete. Journal of Structural Engineering, 114(8):1804–1826.
Mazzoni, S., F. T. McKenna, M. H. Scott, and G. L. Fenves. (2007) Open System for Earthquake Engineering Simulation User Command-Language Manual. Source: http://opensees.berkeley.edu/OpenSees/manuals/usermanual/ OpenSeesCommandLanguageManual.pdf.
Michel, A., Geiker, M.R., Stang, H., Lepech, M. (2013) Integrated modelling of corrosion-induced deterioration in rein-forced concrete structures. EuroCorr 2013. September 1-5, 2013. Estoril, Portugal.
Molina, F., C. Alonso, and C. Andrade. (1993) Cover cracking as a function of rebar corrosion: Part 2 - Numerical model. Materials and Structures, 26(9):532–548.
Organisation for Economic Co-operation and Development OECD. (2011), Strategic Transport Infrastructure Needs to 2030: Main Findings. OECD Futures Project on Transcontinental Infrastructure Needs to 2030/50. Organisation for Economic Co-operation and Development. Pp. 1-21. Source: http://www.oecd.org/futures/infrastructureto2030/49094448.pdf
Ranf, R.T. (2007) Model Selection for Performance-Based Earthquake Engineering of Bridges. Ph.d. dissertation, University of Washington.
Schlangen, E., Copuroglu, O. (2005) “Modelling of deterioration mechanisms in concrete and mortar”. In: 5th International Conference on Computation of Shell and Spatial Structures”. Ramm, E., Wall, W.A., Bletzinger, K.-U., Bischoff, M. (eds.) June 1-4, 2005. Salzburg, Austria.
Stanish, K., R. Hooton, and S. Pantazopoulou. (1999) Corrosion effects on bond strength in reinforced concrete. ACI Structural Journal, 96(6):915–921.
Tapan, M. and R. S. Aboutaha. (2008) Strength Evaluation of Deteriorated RC Bridge Columns. Journal of Bridge Engineering, 13(3):226–236.
Wang, X., and X. Liu. (2004) Modeling bond strength of corroded reinforcement without stirrups. Cement and Concrete Research, 34(8):1331–1339.